Structures, stabilities, electronic and magnetic properties of small RhxMny (x + y = 2–4) clusters

ARTICLE *in* COMPUTATIONAL AND THEORETICAL CHEMISTRY · NOVEMBER 2014

Impact Factor: 1.55 · DOI: 10.1016/j.comptc.2014.08.008

2 AUTHORS, INCLUDING:

Ambrish K. Srivastava
University of Lucknow
72 PUBLICATIONS **168** CITATIONS

SEE PROFILE

Computational and Theoretical Chemistry 1047 (2014) 1–5

Contents lists available at ScienceDirect

Computational and Theoretical Chemistry

journal homepage: www.elsevier.com/locate/comptc

Structures, stabilities, electronic and magnetic properties of small Rh_xMn_y ($x + y = 2–4$) clusters

Ambrish Kumar Srivastava, Neeraj Misra *

Department of Physics, University of Lucknow, Lucknow, Uttar Pradesh 226007, India

ARTICLE INFO

Article history:
Received 26 June 2014
Received in revised form 11 August 2014
Accepted 11 August 2014
Available online 20 August 2014

Keywords:
Rhodium/manganese clusters
Stability
Electronic property
Magnetic moment
Density functional theory

ABSTRACT

The present study investigates Rh_xMn_y clusters for $x + y = 2–4$; x and $y = 1–3$ invoking generalized gradient approximation in density functional theory. The ground state structures are obtained with preferred spin-multiplicities and their stabilities are analyzed by calculating binding energies as well as dissociation energies for various fragmentation channels. Magnetic properties of these clusters are discussed by calculating magnetic moments and spin-density surfaces. Various parameters such as partial charges, dipole moments, HOMO–LUMO energies etc. and density of states spectra are used to explore their electronic properties. We find that all Rh_xMn_y clusters are thermodynamically stable and rhombus Rh_2Mn_2 cluster possesses higher binding energy as compared to other species. The electronic and magnetic properties of Rh_xMn_y clusters vary significantly with the variation in the proportion of Rh and/or Mn atoms. The magnetic moments of Rh range between 0.67 μ_B (in Rh_2Mn_2) and 1.87 μ_B (in Rh_2Mn) and align opposite to that of Mn atoms in case of Rh_2Mn and Rh_3Mn.

1. Introduction

Clusters find important applications in various fields due to their interesting properties which may be quite different than their bulk analog. For instance, bulk rhodium (Rh) is paramagnetic in its fcc phase, whereas, small Rh-clusters possess finite magnetic moments. Rh-clusters have been extensively studied experimentally [1–5] as well as theoretically [6–12]. Many studies have reported the ground-state of Rh_2 dimer to be ferromagnetic with a magnetic moment of 2 μ_B per atom [1,6–8]. On the other hand, the ground-state of Rh_3 trimer has not been determined uniquely. The electron-spin resonance spectra [5] revealed that Rh_3 probably had total magnetic moments of 5 and 7 μ_B. Preliminary investigations by Das and Balasubramanian [10] have reported eight doublet and quartet states within an energy separation of 0.2 eV. Configuration-interaction calculations [11] identified the mixing of several states with multiplicity 6 and 8 in the ground state. However, local-density approximation based calculations [8] resulted in a quartet as the ground-state of Rh_3.

Similarly, manganese (Mn) shows distinguished property of magnetism due to its half-filled 3d orbital. Small clusters of Mn are ferromagnetic, unlike bulk α-Mn which is antiferromagnetic [13,14]. Bobadova-Parvanova et al. [15] studied small Mn_n ($n = 2–7$, 13) clusters and noticed a competition between ferromagnetic and antiferromagnetic ordering of atomic magnetic moments. Furthermore, the measured moments of Mn_n ($n = 5–22$) clusters by Knickelbein [16] suggested that Mn_n clusters are molecular ferrimagnetic in the size range $n = 5–22$. It is widely accepted that due to large energy gap (~8 eV) between the filled 4s and half-filled 3d orbitals, as well as the high promotion energy (~2.14 eV) from $3d^54s^2$ to $3d^64s^1$ of a single Mn atom, small Mn clusters bind with van der Waals' forces. This weak Mn–Mn interaction allows each Mn atom to retain its independent magnetic moment, so it is easy for small Mn-clusters to keep their magnetic moment as large as approximately 5 μ_B per atom.

The present study is devoted to density functional investigations on small clusters of mixed Rh and Mn atoms. The ground-state structures of Rh_xMn_y ($x + y = 2–4$) clusters are obtained with the proportion of x and y varying from 1 to 3 and their stabilities are analyzed. Electronic and magnetic properties of mixed Rh_xMn_y clusters are also calculated and discussed. This is the first report on Rh_xMn_y clusters to the best of our knowledge.

2. Computational methods

All computations are performed using density functional theory (DFT) as implemented in Gaussian 09 program [17]. The generalized gradient approximated (GGA) exchange–correlation functional as devised by Perdew–Burke–Ernzerhof (PBE) [18] is

* Corresponding author.
E-mail address: neerajmisra11@gmail.com (N. Misra).

http://dx.doi.org/10.1016/j.comptc.2014.08.008
2210-271X/

employed in conjunction with Stuttgart–Dresden–Dunning (SDD) basis set. Various initial geometries with all possible spin-multiplicities are fully optimized without any symmetry constraint in the potential energy surface (PES) in order to locate the ground-state structures. Vibrational frequency calculations are repeated for all structures to ensure that they belong to minima in the PES.

In order to check the validity of present computational scheme, we have performed some test calculations on Rh_2 and Mn_2 dimers. The ground-states of Rh_2 (quintet) and Mn_2 (11-et) have been calculated to carry the magnetic moments of 2 μ_B and 5 μ_B per atom, respectively. This fact is consistent with previous assignments [15]. Furthermore, the bond-length of Rh_2 and Mn_2 dimers are calculated as 2.25 Å and 2.62 Å, respectively which are in good agreement with corresponding experimental value of 2.28 Å [1] and already reported values, 2.58–2.84 Å [19–21], respectively. However, the dissociation energies of Rh_2 and Mn_2 calculated to be 1.76 eV/atom and 0.32 eV/atom, respectively are smaller than corresponding experimental values of 2.92 eV/atom [1] and 0.44 ± 0.3 eV/atom [22]. In particular, the binding energy of Rh_2 is fairly underestimated (by 1.12 eV), however, still acceptable as compared to previously reported values, 1.4 eV [2] and 0.85 eV [7].

3. Results and discussion

3.1. Structures and stabilities

The ground-state structures of Rh_xMn_y ($x + y = 2$–4) clusters are displayed in Fig. 1 and respective bond-lengths are also shown. The weak Mn–Mn van der Waals bonds can be easily distinguished as dark black broken lines (in Fig. 1). The ground-state of RhMn is septet with the bond-length (2.27 Å) comparable to that of Rh_2 dimer. $RhMn_2$ (12-et) assumes isosceles triangular geometry, in which Mn–Mn bond-length is increased to 3.11 Å as compared to 2.62 Å in Mn_2 dimer. Thus, the interaction of Rh to Mn_2 dimer further weakens the Mn–Mn bond. Unlike $RhMn_2$, the ground-state of Rh_2-Mn corresponds to the lowest spin (doublet) with equilateral triangular geometry. The ground-state of $RhMn_3$ is triplet in which one of the bond-length is slightly increased as compared to other Rh–Mn and Mn–Mn bond lengths. In fact, $RhMn_3$ can be considered as Mn interacting with $RhMn_2$ triangle which results in slight increase in Rh–Mn and marginal decrease in Mn–Mn bond-lengths. Rh_2Mn_2 takes a rhombus structure with nonet spin as its ground-state in which all Rh–Mn bond-lengths are equalized to 2.39 Å and Mn–Mn is reduced to 2.73 Å as compared to those in $RhMn_2$ and $RhMn_3$ clusters. Like $RhMn_3$, the septet state of Rh_3Mn can be realized by interaction of Rh atom with Rh_2Mn clusters. However, this interaction results in the slight increase in both Rh–Mn and Rh–Rh bond-lengths.

We have calculated vibrational frequencies at PBEPBE/SDD level and found all values to be real, indicating the fact that all optimized structures belong to true minima in the PES. In order to analyze the stabilities of these clusters, we have calculated their binding energies per atom (ΔE) and dissociating energies (D_e) for various fragmentations as below,

$$\Delta E = x\ E[\mathrm{Rh}] + y\ E[\mathrm{Mn}] - E[\mathrm{Rh}_x\mathrm{Mn}_y]/(x+y)$$

$$D_e = E[A] + E[B] - E[\mathrm{Rh}_x\mathrm{Mn}_y]$$

where E[..] represents total electronic energy of respective species including zero point energy calculated at PBEPBE/SDD method, and A and B represent dissociation fragments of Rh_xMn_y clusters.

The calculated ΔE and D_e values are listed in Table 1. All Rh_xMn_y clusters are found to be stable due to ΔE and $D_e > 0$. The ΔE values range between 1.38–2.11 eV/atom. The highest ΔE value corresponds to Rh_2Mn_2 cluster, which appears the most stable among all Rh_xMn_y clusters. The ΔE value of $RhMn_2$ suggests that Mn_2 dimer is significantly destabilized by interaction with Rh atom. As mentioned earlier, this interaction weakens Mn–Mn bond which is also reflected in their preferred dissociation to RhMn + Mn fragments than into Rh + Mn_2 by 2.11 eV. This is in contrast to Rh_2-Mn cluster which prefers to dissociate into Rh_2 + Mn by 0.77 eV. The D_e value of $RhMn_3$ indicates that additional Mn interacts with $RhMn_2$ by 1.31 eV which results in the decrease in overall binding energy of $RhMn_3$ as compared to its neighbors. Similar situation exists in the case of Rh_3Mn cluster, however its ΔE and D_e values are larger than those of $RhMn_3$. Rh_2Mn_2 favors dissociation into two RhMn fragments than into Rh + $RhMn_2$ and Mn + Rh_2Mn by 0.48 eV and 0.12 eV, respectively.

3.2. Electronic and magnetic properties

Rh and Mn possess the outer electronic configurations of $4d^85s^1$ and $3d^54s^2$, so their ground-state magnetic moments are 1 μ_B and 5 μ_B, respectively. The interaction of Rh with Mn does not affect the

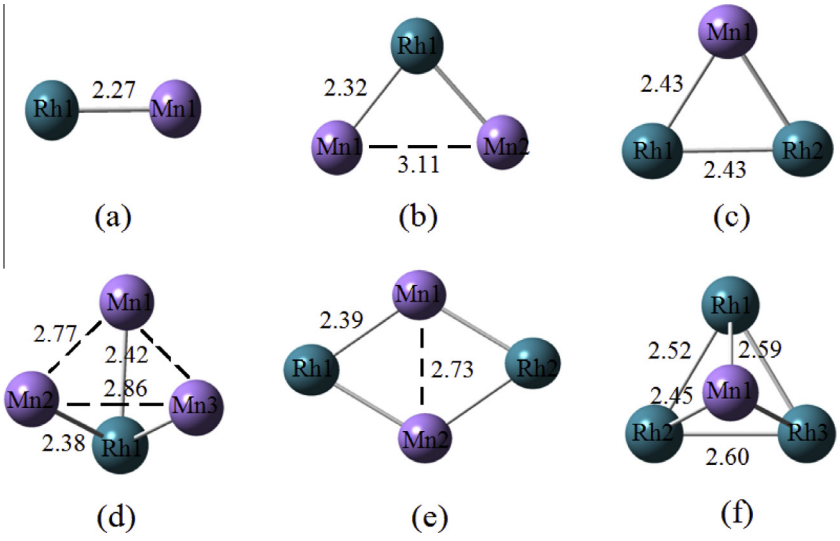

Fig. 1. Ground-state equilibrium geometries of Rh_xMn_y ($x + y = 2$–4) clusters. Mn–Mn (van der Waals bonding) are shown by broken black lines and all bond-lengths (in Å) are also given.

Table 1
Binding energy (ΔE) and dissociation energies (D_e) for various fragments for Rh_xMn_y ($x + y = 2–4$) clusters calculated at PBEPBE/SDD method.

Clusters	ΔE (eV/atom)	Dissociation fragments [D_e (eV)]
RhMn	1.38	Rh + Mn [2.76]
$RhMn_2$	1.67	RhMn + Mn [2.27], Rh + Mn_2 [4.38]
Rh_2Mn	1.79	RhMn + Rh [2.63], Rh_2 + Mn [1.86]
$RhMn_3$	1.59	RhMn + Mn_2 [2.94], $RhMn_2$ + Mn [1.31], Rh + Mn_3 [4.03]
Rh_2Mn_2	2.11	2 RhMn [2.94], $RhMn_2$ + Rh [3.42], Rh_2Mn + Mn [3.06], Rh_2+Mn_2 [4.27]
Rh_3Mn	1.83	RhMn + Rh_2 [3.64], Rh_2Mn + Rh [2.54], Rh_3 + Mn [2.94]

Table 2
Magnetic moments (μ) of Rh_xMn_y ($x + y = 2–4$) clusters calculated at PBEPBE/SDD method.

Clusters	Magnetic moments (μ_B)						
	μ(Total)	$\mu(Rh_1)$	$\mu(Rh_2)$	$\mu(Rh_3)$	$\mu(Mn_1)$	$\mu(Mn_2)$	$\mu(Mn_3)$
RhMn	6	1.22			4.77		
$RhMn_2$	11	0.73			5.14	5.14	
Rh_2Mn	1	−1.87	−1.87		4.74		
$RhMn_3$	2	0.79			−5.73	4.26	4.26
Rh_2Mn_2	8	−0.67	−0.67		4.67	4.67	
Rh_3Mn	6	1.03	0.07	0.07	4.86		

magnetic states and both maintain their individual magnetism which is reflected in their magnetic moments in RhMn. In $RhMn_2$, there is a ferromagnetic coupling between Mn atoms each with moments of 5.14 μ_B as, whereas Rh possesses the magnetic moment of 0.73 μ_B. Likewise in Rh_2Mn cluster, there is ferromagnetic alignment between Rh atoms with 1.87 μ_B and Mn has magnetic moment of 4.74 μ_B. Note that both Mn_2 and Rh_2 dimers are ferromagnetic with the magnetic moments of 5 μ_B and 2 μ_B per atom, respectively. However, the interaction of Mn with Rh_2 causes to change the direction of its moments such that the total magnetic moment of Rh_2Mn is reduced to 1 μ_B as compared to 4 μ_B of Rh_2 dimer.

In $RhMn_3$, there is a ferrimagnetic alignment among Mn atoms resulting in a total magnetic moment of 2 μ_B in which Rh atom contributes by 0.79 μ_B. This fact is in contrast to Mn_3 trimer in which all Mn atoms align ferromagnetically with a magnetic moment of 5 μ_B per atom [20]. Just as in $RhMn_2$, there are also ferromagnetic couplings between Rh as well as Mn atoms in Rh_2Mn_2 cluster. However, these couplings result in a total magnetic moment of 8 μ_B which is smaller than that of $RhMn_2$ (11 μ_B). This is due to reversal of the magnetic moment of Rh, as in the case of Rh_2Mn cluster. The total magnetic moment of Rh_3Mn cluster is 6 μ_B, which is mainly contributed by one Rh (1.03 μ_B) and Mn (4.86 μ_B), same as in RhMn cluster.

The magnetic properties of Rh_xMn_y clusters can further be explained by spin-density surfaces shown in Fig. 2. In color coding scheme, blue and green represent the excess of spin up (↑) and spin down (↓) electrons, respectively. Consequently, these lead to the positive and negative magnetic moments. For instance, in Rh_2Mn cluster, the blue region is localized on Mn atoms and green is delocalized over Rh atoms which results in negative magnetic moments of Rh atoms (see Table 2). Similarly in Rh_2Mn, there is an excess of spin down electrons on Rh sites and spin up electrons on Mn site resulting in negative and positive magnetic moments, respectively.

The partial atomic charges on Rh and Mn atoms in Rh_xMn_y clusters are obtained by various population analyses viz. Mulliken, natural bonding orbital (NBO) and Hirshfeld schemes. Mulliken population analysis (MPA) is the most common procedure which makes use of the density matrix, assigning diagonal terms belonging to the basis set used for a given atom to that atom [23]. It has, therefore, a strong dependence on the basis set used [24] which restricts its usefulness. An improved procedure employing NBO analysis has been very popular due to its less basis dependency and assignment of maximum possible occupancy to each atomic orbital [25]. The Hirshfeld scheme has been known to yield an optimal partitioning of electron density and seem to work efficiently as compared to MPA [26]. The calculated atomic charges are listed in Table 3. One can note that the MPA assigns positive charges to Rh atoms, whereas in NBO and Hirshfeld schemes, almost all Rh charges are negative. Hence, the MPA charges do not seem to be reliable when compared with NBO or Hirshfeld. However, there are significant variations in the magnitudes of Hirshfeld and NBO charges (see Table 3). So, we have calculated atomic polar tensor (APT) derived charges [27] (also listed in Table 3) and compared with Hirshfeld and NBO charges. We find that APT calculated magnitudes of charges are higher than Hirshfeld but smaller than NBO. It can be expected due to the fact that NBO assigns the maximum

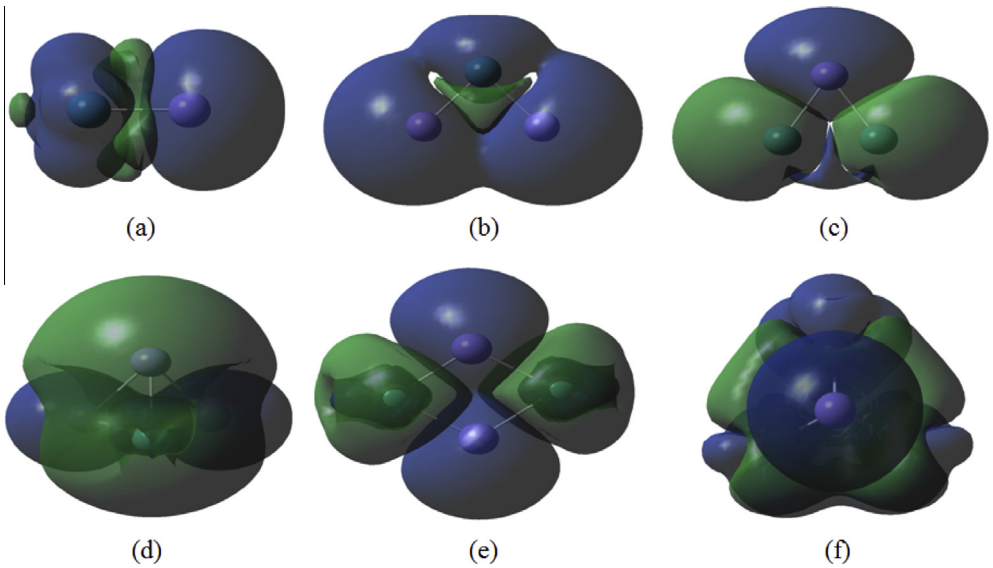

Fig. 2. Spin-density surfaces of (a) RhMn, (b) $RhMn_2$, (c) Rh_2Mn, (d) $RhMn_3$, (e) Rh_2Mn_2, and (f) Rh_3Mn clusters with an isovalue of 0.0004 a.u.

Table 3
Partial atomic charges (in e) on Rh and Mn in Rh_xMn_y clusters calculated by Mulliken, NBO, Hirshfeld and APT schemes.

Clusters	Mulliken charges		NBO charges		Hirshfeld charges		APT charges	
	q(Rh)	q(Mn)	q(Rh)	q(Mn)	q(Rh)	q(Mn)	q(Rh)	q(Mn)
RhMn	+0.10	−0.10	−0.24	+0.24	−0.04	+0.04	−0.11	+0.11
$RhMn_2$	+0.27	−0.13	−0.62	+0.31	−0.06	+0.03	−0.07	+0.03
Rh_2Mn	+0.10	−0.21	−0.25	+0.50	−0.06	+0.12	−0.13	+0.26
$RhMn_3$	+0.47	−0.20	−0.77	+0.26	+0.01	−0.01	−0.08	+0.03
Rh_2Mn_2	+0.22	−0.22	−0.45	+0.45	−0.03	+0.03	−0.10	+0.10
Rh_3Mn	+0.06	−0.18	−0.20	+0.55	−0.04	+0.08	−0.12	+0.35

Table 4
Dipole moment, energies of HOMO (E_H), LUMO (E_L) and their energy gap (E_g) in spin up and spin down state of Rh_xMn_y ($x + y = 2–4$) clusters calculated at PBEPBE/SDD method. All energy values are measured in eV.

Clusters	Spin up (↑) state			Spin down (↓) state			Dipole moment (D)
	E_H	E_L	E_g	E_H	E_L	E_g	
RhMn	−4.54	−3.11	1.44	−4.24	−3.85	0.38	1.25
$RhMn_2$	−3.79	−3.02	0.78	−4.06	−2.88	1.18	1.06
Rh_2Mn	−4.39	−4.01	0.38	−3.36	−2.99	0.37	2.10
$RhMn_3$	−4.73	−3.70	1.04	−3.69	−2.90	0.79	1.43
Rh_2Mn_2	−4.03	−3.93	0.10	−4.23	−2.78	1.46	0.00
Rh_3Mn	−4.55	−2.68	1.87	−4.47	−2.37	2.09	1.93

possible occupancy to each atom, as mentioned earlier. We can refer to NBO charges in order to discuss the electron distribution in Rh_xMn_y clusters, at least qualitatively. As mentioned earlier, the NBO charges on Rh are all negative, whereas those of Mn are positive. Thus, all Rh atoms accept electrons from Mn, which is expected due to half-filled 3d orbitals of Mn. This electron-transfer increases with the increase either in Mn atoms ($RhMn_2$, $RhMn_3$ etc.) or in Rh atoms (Rh_2Mn, Rh_3Mn etc.). The dipole moment gives a signature of the geometry and charge distribution of clusters. Asymmetry in the charge distribution corresponds to the higher dipole moment, increasing the polarity within the species. From Table 4, it is evident that the higher dipole moment (2.10 D) of

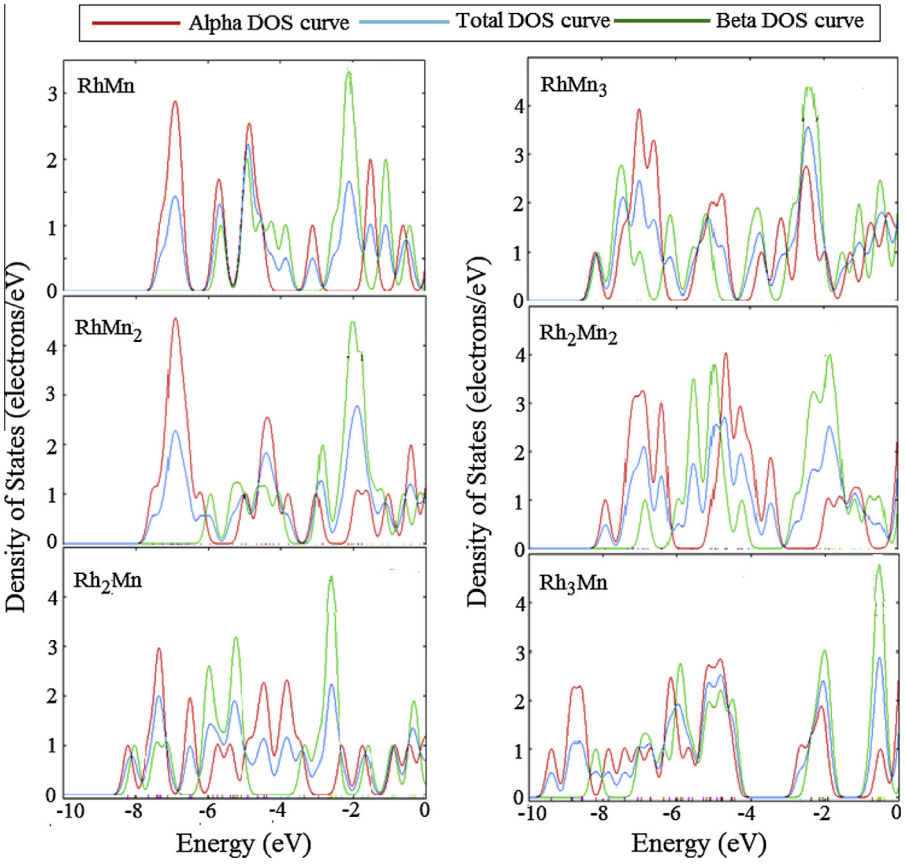

Fig. 3. Density-of-States (DOS) spectra of Rh_xMn_y ($x + y = 2–4$) clusters calculated by PBEPBE/SDD method. Note that total DOS curves are scaled by 0.5.

Rh_2Mn makes it more polar, which is also reflected in partial atomic charges of Rh_2Mn. On the other hand, the dipole moment is completely vanished in Rh_2Mn_2 due to symmetric distribution of charges over all atoms. Note that all atoms in Rh_2Mn_2 cluster possess the partial charges of ±0.45 e.

Table 4 also lists the energies of the highest occupied molecular orbital (HOMO) (E_H), lowest unoccupied molecular orbital (LUMO) (E_L) and their energy gap (E_g) of spins up (↑) and spins down (↓) states. One can notice that all E_L values are negative, further implying the stabilities of clusters. Within the framework of Koopmans' theorem, the negative of E_H and E_L approximate the ionization potential (IP) and electron affinity (EA), respectively. Therefore, higher E_H and E_L correspond to the lower IP and EA. It is well known that the extraction (addition) of an electron from (to) chemical species is favored by their low IP (high EA). Consequently, the values of E_H and E_L can be useful in deciding whether this electron comes from (goes to) spin up or spin down state. For instance, the E_H and E_L values of Rh_2Mn cluster suggest that an electron can be easily removed from spin down state but can be added with spin up. It may be expected due to the fact that the last electron in the HOMO of Rh_2Mn is unpaired with spin down.

The importance of HOMO and LUMO lies in the fact that these are the orbitals which mainly participate in chemical reactions or interactions with other species. Their energy gap (E_g) is an important factor deciding the chemical reactivity of molecular species. The species with smaller E_g values may interact easily and hence, they become chemically more reactive. For instance, the E_g value of RhMn suggests that it is more reactive than $RhMn_2$, which is also reflected in its lower binding energy as compared to that of $RhMn_2$ (see Table 1).

In order to further explain the electronic and magnetic properties of Rh_xMn_y clusters, we have plotted their total density-of-states (DOS) spectra in Fig. 3. The DOS curves of spin up (alpha) and spin down (beta) electrons are also included. We consider the case of Rh_2Mn_2 cluster in which Rh and Mn atoms possess the magnetic moments of 0.67 μ_B and 4.67 μ_B per atom, in mutually opposite directions. From spin-density plot in Fig. 2, it is apparent that the electrons of Mn and Rh align with spins up and spins down, respectively. The DOS spectra show that the HOMO of Rh_2Mn_2 cluster corresponds to the alpha- and beta-DOS values of 2.2 and 0.3 per eV, which results in magnetic moments of 9.3 μ_B due to spin up electrons and 1.3 μ_B spin down electrons. These up and down moments are equally shared by Mn and Rh atoms, giving a total magnetic moment of 8 μ_B (see Table 2).

4. Conclusion

Using density functional PBEPBE/SDD method, we have discussed the structures and stabilities of Rh_xMn_y clusters for $x + y = 2–4$. In general, all Rh_xMn_y species are found to be thermodynamically stable and the rhombus Rh_2Mn_2 cluster has been found to possess higher binding energy as compared to others. The electronic and magnetic properties of Rh_xMn_y clusters are systematically studied. In all cases, Mn atoms have been found to maintain their atomic moments of 5 μ_B, due to their participation in weak bonding. With the increase in the proportion of x and/or y, we have noticed the ferromagnetic and ferrimagnetic alignments of atomic moments of Rh and Mn. A reversal in the direction of magnetic moments of Rh atoms has been found in case of Rh_2Mn and Rh_3Mn. Partial atomic charges, dipole moments, and HOMO–LUMO energies are calculated to discuss the electronic properties. Spin-densities and density-of-states curves are also plotted in order to explain the electronic and magnetic properties of Rh_xMn_y clusters.

Acknowledgement

A.K. Srivastava acknowledges Council of Scientific and Industrial Research (CSIR), India for providing a research fellowship [Grant No. 09/107(0359)/2012-EMR-I].

References

[1] K.A. Gingerich, D.L. Cocke, Thermodynamic confirmation for the high stability of gaseous TiRh as predicted by the Brewer–Engel metallic theory and the dissociation energy of diatomic rhodium, J. Chem. Soc., Chem. Commun. 1 (1972). 536–536.
[2] H. Wang, H. Haouari, R. Craig, Y. Liu, J.R. Lombardi, D.M. Lindsay, Spectroscopy of mass-selected rhodium dimers in argon matrices, J. Chem. Phys. 106 (1997) 2101–2104.
[3] A.J. Cox, J.G. Louderback, L.A. Bloomfield, Experimental observation of magnetism in rhodium clusters, Phys. Rev. Lett. 71 (1993) 923–926.
[4] A.J. Cox, J.G. Louderback, S.E. Apsel, L.A. Bloomfield, Magnetism in 4d-transition metal clusters, Phys. Rev. B 49 (1994) 12295–12298.
[5] R.J. Van Zee, Y.M. Hamrick, S. Li, W. Weltner Jr., ESR of Co, Rh, Ir trimers and diatomic ions, Chem. Phys. Lett. 195 (1992) 214–220.
[6] K. Balasubramanian, D.W. Liao, Spectroscopic properties of low-lying electronic states of rhodium dimer, J. Phys. Chem. 93 (1989) 3989–3992.
[7] F. Illas, J. Rubio, J. Canellas, J.M. Ricart, Electronic structure of Rh, RhH, and Rh_2 as derived from abinitio (configuration interaction) calculations, J. Chem. Phys. 93 (1990) 2603.
[8] Y. Jinlong, F. Toigo, W. Kelin, Structural, electronic, and magnetic properties of small rhodium clusters, Phys. Rev. B 50 (1994) 7915–7924.
[9] S.K. Nayak, S.E. Weber, P. Jena, K. Wildberger, R. Zeller, P.H. Dederichs, V.S. Stepanyuk, W. Hergert, Relationship between magnetism, topology, and reactivity of Rh clusters, Phys. Rev. B 56 (1997) 8849–8854.
[10] K.K. Das, K. Balasubramanian, Potential energy surfaces of eight low-lying electronic states of Rh3, J. Chem. Phys. 93 (1990) 625–632.
[11] D. Dai, K. Balasubramanian, High-spin electronic states of the rhodium trimer (Rh_3), Chem. Phys. Lett. 195 (1992) 207–213.
[12] B.V. Reddy, S.N. Khanna, B.I. Dunlap, Giant magnetic moments in 4d clusters, Phys. Rev. Lett. 70 (1993) 3323–3326.
[13] M.B. Knickelbein, Experimental observation of superparamagnetism in manganese clusters, Phys. Rev. Lett. 86 (2001) 5255–5257.
[14] R.J. Van Zee, W. Waltner Jr., The ferromagnetic Mn^{+2} molecule, J. Chem. Phys. 89 (1988) 4444.
[15] P. Bobadova-Parvanova, K.A. Jackson, S. Srinivas, M. Horoi, Emergence of antiferromagnetic ordering in Mn clusters, Phys. Rev. A 67 (2003) 061202.
[16] M.B. Knickelbein, Magnetic ordering in manganese clusters, Phys. Rev. B 70 (2004) 014424–014428.
[17] M.J. Frisch, G.W. Trucks, H.B. Schlegel, G.E. Scuseria, M.A. Robb, J.R. Cheeseman, G. Scalmani, V. Barone, B. Mennucci, G.A. Petersson, H. Nakatsuji, M. Caricato, X. Li, H.P. Hratchian, A.F. Izmaylov, J. Bloino, G. Zheng, J.L. Sonnenberg, M. Hada, M. Ehara, K. Toyota, R. Fukuda, J. Hasegawa, M. Ishida, T. Nakajima, Y. Honda, O. Kitao, H. Nakai, T. Vreven, J.A. Montgomery, Jr., J.E. Peralta, F. Ogliaro, M. Bearpark, J.J. Heyd, E. Brothers, K.N. Kudin, V.N. Staroverov, T. Keith, R. Kobayashi, J. Normand, K. Raghavachari, A. Rendell, J.C. Burant, S.S. Iyengar, J. Tomasi, M. Cossi, N. Rega, J. M. Millam, M. Klene, J.E. Knox, J.B. Cross, V. Bakken, C. Adamo, J. Jaramillo, R. Gomperts, R.E. Stratmann, O. Yazyev, A.J. Austin, R. Cammi, C. Pomelli, J.W. Ochterski, R.L. Martin, K. Morokuma, V.G. Zakrzewski, G.A. Voth, P. Salvador, J.J. Dannenberg, S. Dapprich, A.D. Daniels, O. Farkas, J.B. Foresman, J.V. Ortiz, J. Cioslowski, D.J. Fox, Gaussian 09, Revision B.01, Gaussian Inc., Wallingford CT, 2010.
[18] J.P. Perdew, K. Burke, M. Ernzerhof, Generalized gradient approximation made simple, Phys. Rev. Lett. 77 (1996) 3865–3868.
[19] S.K. Nayak, B.K. Rao, P. Jena, Equilibrium geometries, electronic structure and magnetic properties of small manganese clusters, J. Phys.: Condens. Matter 10 (1998) 10863–10877.
[20] M. Kabir, A. Mookerjee, D.G. Kanhere, Structure, electronic properties, and magnetic transition in manganese clusters, Phys. Rev. B 73 (2006) 224439.
[21] G.L. Gutsev, M.D. Mochena, P. Jena, C.W. Bauschlicher Jr., H. Partridge III, Periodic table of 3d-metal dimers and their ions, J. Chem. Phys. 121 (2004) 6785–6797.
[22] M.D. Morse, Clusters of transition-metal atoms, Chem. Rev. 86 (1986) 1049–1109.
[23] R.S. Mulliken, Criteria for the construction of good self-consistent-field molecular orbital wave functions, and the significance of LCAO–MO population analysis, J. Chem. Phys. 36 (1962) 3428.
[24] R.S. Mulliken, P. Politzer, Comparison of two definitions of atomic charge, as applied to hydrogen fluoride, J. Chem. Phys. 55 (1971) 5135.
[25] A.E. Reed, R.B. Weinstock, F. Weinhold, Natural population analysis, J. Chem. Phys. 83 (1985) 735–746.
[26] F.L. Hirshfeld, Bonded-atom fragments for describing molecular charge densities, Theoret. Chim. Acta 44 (1977) 129–138.
[27] J. Cioslowski, A new population analysis based on atomic polar tensors, J. Am. Chem. Soc. 111 (1989) 8333–8336.